Book Chapter

Chemical-Induced Denaturation of Myoglobin Under Crowded Environment

Khalida Nasreen[1#], Zahoor Ahmad Parray[1], Ikramul Hasan[2] and Asimul Islam[1*#]

[1]Centre for Interdisciplinary Research in Basic Sciences, Jamia Millia Islamia, India
[2]Department of Basic Medical Science, Faculty of Applied Medical Sciences, Al-Baha University, KSA

[#]These authors contributed equally to this work.

***Corresponding Author:** Asimul Islam, Centre for Interdisciplinary Research in Basic Sciences, Jamia Millia Islamia, Jamia Nagar, New Delhi 110025, India

Published **July 06, 2020**

This Book Chapter is a republication of an article published by Asimul Islam, et al. at Biomolecules in March 2020. (Nasreen, K.; Parray, Z.A.; Ahamad, S.; Ahmad, F.; Ahmed, A.; Freeh Alamery, S.; Hussain, T.; Hassan, M.I.; Islam, A. Interactions Under Crowding Milieu: Chemical-Induced Denaturation of Myoglobin is Determined by the Extent of Heme Dissociation on Interaction with Crowders. Biomolecules 2020, 10, 490.)

How to cite this book chapter: Khalida Nasreen, Zahoor Ahmad Parray, Ikramul Hasan, Asimul Islam. Chemical-Induced Denaturation of Myoglobin Under Crowded Environment. In: Song Guo Zheng, editor. Prime Archives in Molecular Biology. Hyderabad, India: Vide Leaf. 2020.

Conflict of interest: There is no conflict of interest from authors.

Acknowledgements: This work was supported by the Council of Scientific and Industrial Research (CSIR), India (37(1603)/13/EMR-II) &(37(1604)/13/EMR-II), FIST Program (SR/FST/LSI-541/2012), Indian Council of Medical Research (ICMR)BIC/12(16)/2014 and the Science and Engineering Research Board (SERB) India (SR/FT/LS-48/2010).FA is grateful to Indian National Science Academy for the award of Senior Scientist Position.KN acknowledges the financial support from UGC-MANF-JRF/SRF. ZAP is grateful for the award of SRF from ICMR (45/39/2018-BIO/BMS).

Abstract

Generally, *in vivo* function and structural changes are studied by probing proteins in a dilute solution under *in vitro* conditions, which is believed to be mimicking proteins in intracellular milieu. Earlier, thermal-induced denaturation of myoglobin in the milieu of crowder molecule showed destabilization of the protein. Destabilization of protein by thermal-induced denaturation involves a large extrapolation, so, that the reliability is questionable. This led us to measure the effects of macromolecular crowding on its stability by chemical-induced denaturation of the protein using probes like circular dichroism and absorption spectroscopy in the presence of dextran 70 and ficoll 70 at various pHs (acidic: 6.0, almost neutral: 7.0 and basic: 8.0). Observations showed that the degree of destabilization of myoglobin was greater due to ficoll 70 as compared to that of dextran 70 so it can be understood that the nature of crowder or the shape of crowder has important role towards stability of proteins. Also, the degree of destabilization was observed pH dependent. Furthermore, isothermal titration calorimetry and molecular docking studies was confirmed that both the crowders (ficoll 70 and dextran 70) bind to heme moiety of myoglobin and single binding site was observed for each.

Keywords

Macromolecular Crowding; Protein Stability; Chemical-Induced Denaturation; Myoglobin; Ficoll; Dextran; Isothermal Titration Calorimetry

Introduction

Generally, it is assumed that folding methods and biophysical & structural properties of an isolated protein monitored in dilute solutions (*in vitro*) are similar to the cellular conditions (*in vivo*). However, there are two major differences between *in vitro* and *in vivo* protein folding. First, there is complete machinery available in the cell for proper folding of the protein like chaperones, etc. In the case of small proteins like cytochrome c, myoglobin, lysozyme and ribonuclease A, chaperones are not required and the folding of protein is reversible and quick, even in absence of such folders. The second and important difference is the presence of highly crowded intracellular environment due to huge quantity of insoluble and soluble biomolecules, which comprises of proteins, nucleic acid, carbohydrates, osmolytes, ribosomes, and architecture of a cell [1].

Crowding can have significant effect on structure, stability, functional activity, and aggregation of proteins; it may affect kinetics of protein folding, protein-protein interactions, and other complex physiological processes undergoing in a cell [2,3]. Since the intracellular environment is highly crowded, it becomes very imperative and interesting to know how protein folds and function in the cellular environment. Various natural and artificial crowder molecules are used with the purpose to investigate the structural, functional changes and type of interactions induced by crowding, in order to mimic cell like conditions [2,4]. Since, the cellular environment is composed of various biomolecules which differ in shape, size and chemical nature [5], thus, crowders having different shape, size and nature were used in order to study the effect of crowding [6,7]. The dependence of crowding effect on the concentration, size, shape and nature of crowding agents are very important attributes which must be considered while studying protein folding [8].

Many findings are there to demonstrate the crowding effect on the conformations of proteins [9-17]. In some cases, crowding agents have significantly altered the structural contents of several proteins while the conformational properties of some proteins have remained unaffected in the presence of crowding environment. The secondary structural content of *D. desulfuricans* flavodoxin [11], apoflavodoxin [10], bovine pancreatic RNase A [18], holo α-lactalbumin from bovine milk [18], rabbit muscle creatine kinase [14] and *B. burgdorferi* VIsE [13] in their native state, increased due to ficoll 70 and/or dextran 70 and is concentration dependent, however thermally and chemically denatured state remained unaffected. In contrast, the secondary structure of the monomeric multi-copper oxidase Fet3pfrom *Saccharomyces Cerevisiae* [19] and lysozyme from hen egg white [18] were not affected by ficoll 70 [18,19] and dextran 70 [20], respectively. Conversely, the reports had shown that there was decrease in the secondary structure of rabbit muscle creatine kinase due to dextran 70 [21]. In addition, it has been demonstrated that dextran 20 shows unique character in the unfolded or partially folded proteins including variant of *Streptococcusmagnus* immunoglobulin G binding domain of protein L, [16], *S. Cerevisiae* Fet3p [19] and F10C/W74F small ribosomal variant protein (S16) 15], leads to increase in their secondary structures. Though, dextran 20 was unable to show such change in the secondary structure of apoflavodoxin from *A. vinelandii* [12] and ubiquitin, but significant changes were observed in its denatured state [22].

Most of the times, the phenomenon of macromolecular crowding increases the thermodynamic stability of proteins [9-18,20,23-33]. However, the recent study of Ashima Malik & collaborators [34], observed that effects of the crowding agents on myoglobin leads to deviation from the general belief that crowding agents (synthetic) are always stabilizing in nature. They did thermo-chemical denaturation experiments using urea (different concentrations) in the presence of crowders. They showed that ficoll 70 particularly destabilizes Mb. Both chemical- and heat-induced denaturation revealed different effects on the unfolded ensemble of Mb in presence of the crowders. The concentration of 200 mg/ml of the crowders was observed using heat-induced

denaturation method, to have destabilizing effect on Mb. The data acquired from the heat-induced chemical denaturation curves involves a long data extrapolation measured in the range of temperature away from the 25 ^{o}C and this range of extrapolation increases whilst co-solutes are taken. Thus ΔG_D^0 value obtained may shows some error, which shows deviation in T_m (the midpoint of thermal denaturation) in the presence of co-solutes [35]. In this work, we have performed experiments at 25 ^{o}C at different pH values using different concentrations of ficoll 70 and dextran 70 on Mb, using more accurate method i.e., under chemical (GdmCl and urea)-induced denaturation.

In this study, the effect of ficoll 70 and dextran 70 was observed on the structure and stability of myoglobin (Mb) at variable pH values (6.0, 7.0, and 8.0) under chemical-induced denaturing conditions (GdmCl and urea) using specific probes of absorption and circular dichroism (CD) spectroscopy. Besides, interaction studies of ficoll 70 and dextran 70, with Mb was investigated using isothermal titration calorimetry (ITC) and molecular docking studies.

Materials and Methods

Materials

Lyophilized myoglobin (horse heart), ficoll 70, dextran 70 and sodium salt of cacodylate were procured from Sigma Aldrich Private Ltd. (USA). Potassium ferricyanide, ethylene diaminetetraacetic acid (EDTA), potassium chloride (KCl), hydrochloric acid (HCl) and sodium hydroxide (NaOH) pellets were bought from Merck (India). Guanidinium chloride (GdmCl) and ultrapure urea were procured from ICN Biomedical (USA). Filters (0.22 µm pore size) were procured from Millipore Corporation and parafilm from American National Co., Chicago, USA.

Methods

Preparation of Protein Solutions

Stock solution of Mb (5 mg/ml) was prepared in 0.1 M KCl. The solution was then oxidized using 0.01% potassium ferricyanide

($K_3Fe(CN)_6$) [36]. In order to remove excess of potassium ferricyanide and additional salts present in the protein (lyophilized form), the solution prepared was dialyzed comprehensively against changes of 0.1 M KCl in conditions of pH 7.0 and at 4 ^oC. Solution of protein was then filtered using 0.22 µm Millipore filter paper. Concentration of Mb was determined using molar absorption coefficient value of 171,000 $M^{-1}cm^{-1}$ at wavelength 409 nm [37].

Denaturant Stock Solution Preparations

Required amount of denaturants (GdmCl and urea) were dissolved in the desirable buffers used in the experiments (0.1 M KCl and 0.05 M cacodylic acid). The pHs of these solutions were then adjusted using NaOH or HCl as per used in the experiments. The solutions were then filtered through Whatman filter paper no. 1. The Abbe refractrometer was then used to check refractive index, and plotted using the tabulated values of the refractive index reported for GdmCl by Nozaki [38] and for urea by Pace [39]. GdmCl stock solution was stored for further use while urea stock solution was always prepared fresh because urea tends to decompose forming cyanate and ammonia ion [40], reacts with sulphydryl groups and ammonia of the protein leads irreversible inactivation [41].

Preparation of Crowder Stock Solution

Concentrated stock solution of crowders (ficoll and dextran) was prepared by dissolving required amount of crowder in distilled water. KCl and cacodylic acid were added to the solution in order to get a final concentration of 0.1 M and 0.05 M respectively. The NaOH or HCl were used to equilibrate pH of the solutions as required in the work. In order to remove the impurities, the solutions were filtered using Whattman filter paper and then stored at 4 ^0C. The concentration of the crowders i.e. ficoll 70 and dextran 70, were calculated using the reported refractive increment value [42,43]. For experiment measurements, the each solution sample was thoroughly mixed and overnight incubation was done at room temperature.

Spectral Measurements and Analysis of Isothermal Transition Curves

Absorption Spectroscopy:

Spectral measurements were carried out in Jasco-660 UV/Visible spectrophotometer equipped with Peltier type temperature controller (ETCS-761), using cuvette of 1 cm path length. Temperature of the cell was set at 25 ± °C by thermo-stated circulating water bath. 3-4 µM of the protein concentration was used for the spectral measurements, which were carried in the wavelength range of 450-350 nm. Correction of baseline was carried out continuously using the working buffer. The spectrum of the native protein was subtracted from that of the denatured protein in order to get the difference spectrum. Wavelength at which maximum change was observed in the difference spectrum was further used to monitor the denaturation curves i.e. 409 nm. The raw data was converted into molar absorption coefficient, ε using the relation:

$$A = \varepsilon c l \qquad (1)$$

where A is the absorbance, c is molar concentration of the protein, l is the path length of the cuvette in cm and ε is molar absorption coefficient. The change in the absorption coefficient ($\Delta\varepsilon_{409}$) was used as probe to plot denaturation curves at all concentrations.

Far-UV Circular Dichroism (CD) Spectroscopy:

Circular dichroism studies were made using Jasco J-1500 CD spectropolarimeter equipped with a Peltier type temperature controller attached to circulating water bath (MCB-100), using a cell of path length 0.1 cm. Protein concentration used for CD measurements was 6-7 µM. The equipment was regularly calibrated using D-10 camphorsulphonic acid. Baseline correction was done using buffer. 3-5 accumulations of each sample including the baseline were taken in order to improve the CD signals, which is the average of each spectrum. Nitrogen gas was continuously flushed at the rate of 3-5 lit/min inside the cuvette chamber in order to minimize the noise level. Far-UV

CD spectra were scanned in the range of 250–200 nm. The raw data from CD (milli degree) were changed into mean residual ellipticity completely using the relation [44]:

$$[\theta]_\lambda = M_0\theta_\lambda/10lc \qquad (2)$$

where θ_λ is the ellipticity observed in millidegrees at wavelength of λ , l is the path length of the cuvette in centimeters, M_0 and c are the mean residue weight and the concentration of the protein respectively. The ellipticity at 222 nm, $[\theta]_{222}$ was used as probe to plot denaturation curves at all concentrations to monitor secondary structure.

Reversibility of denatured Mb was checked by measuring optical property using high concentration of denaturant, and then dialyzing it with respective buffer.

Analysis of Isothermal Denaturation Curves:

Analysis of isothermal denaturation curves was done in order to find out the stability of protein in the absence and presence of co-solute. Protein stability is defined as the change in Gibb's free energy when an unfolded polypeptide chain folds into its stable native conformation.

$$\text{N (native conformation)} \underset{K_D}{\overset{\Delta G_D}{\longleftrightarrow}} \text{D (denatured conformation)}$$

$$\Delta G = G_D - G_N \qquad (3)$$

$$K_D = [D] / [N] \qquad (4)$$

Analysis of isothermal transition curves was based on two assumptions: (1) the isothermal denaturation process is reversible and (2) the denaturation proceeds through two-state mechanism, having equilibrium between

N (native conformation) ↔ **D** (denatured conformation)

The change in Gibb's free energy (ΔG_D) for folding-unfolding was analyzed using the relation:

$$\Delta G_D = -RT \ln K_D \quad (5)$$

where, R is the gas constant (1.98 cal deg^{-1} mol^{-1}) and T is the absolute temperature in Kelvin (K) and K_D can be computed using the relation:

$$K_D = f_D / (1 - f_D) = (y - y_N) / (y_D - y) \quad (6)$$

where, y is the optical property measured at the specific concentration of denaturant, y_N and y_D denotes the native and denatured states respectively. These are points in the transition region, obtained by linear extrapolation of the pre- and post-transition region and attained under the same experimental conditions where y has been observed.

$\Delta G_{N\leftrightarrow D}$ was plotted against the molar concentration of each denaturant and $\Delta G_D°$ was estimated from the least square analysis using the relation:

$$\Delta G_D = \Delta G_D° - m[d] \quad (7)$$

where, $\Delta G^{\circ}_{N\leftrightarrow D}$ is the value of ΔG_D in the absence of denaturant and m is the slope of the line i.e., $(\partial \Delta G_D / \partial [d])_{T, P}$ and [d], the molar concentration of denaturant. The transition curve midpoint, C_m was analyzed from $C_m = \Delta G_D°/m$.

Alternatively, the entire equilibrium transition curve was fitted and analyzed to a two state unfolding model in order to get the values of $\Delta G_D°$, m and C_m using the relation given by Santoro and Bolen:

$$y(d) = \frac{yN\,(d) + yD\,(d)\ X\ Exp[-(\Delta GD° + m\,[d])\ /\ RT]}{1 + Exp\,[-(\Delta GD° + m\,[d])\ /\ RT]} \quad (8)$$

where, y(d) is the optical property observed at a specific concentration of denaturant, y_N and y_D are the native and denatured state optical properties respectively in similar

experimental conditions where $y(d)$ was measured. $\Delta G_D°$ is change in Gibb's free energy of native protein, m is the slope of $\partial\Delta G_D$ versus $\partial[d]$ plot, T is the temperature in Kelvin and R is the universal gas constant.

Isothermal Titration Calorimetry (ITC)

ITC experiments were performed in MicroCal VP-ITC system at pH 7.0 and 25 °C. The concentration of dextran 70 and Mb were taken in the ratio of 1:10 respectively. 2 ml crowder solution (200 µM) was taken inside the sample cell and in injection syringe 280 µl of protein solution (20 µM) was loaded. Stirring speed of the syringe was 372 rpm. There was negligible heat of dilution between buffer and the crowders and baseline was subtracted from the raw data (protein and crowders) to get final results. MicroCal ORIGIN software was used in order to analyze the data and find out the binding model that could be best fitted to the data. Raw data were processed using Origin version 7.0 software and was fitted by one Site model using Microcal.

Computational Methods

In silico assessment of binding between ficoll 70 or dextran 70 with Mb (PDB ID: 1ymb) was done by means of AutoDock4, software for docking and maestro visualizer (schrodinger-version 10.6), 2D interaction plot [45]. The preparation of input file was done by chemdraw and MM2 force field (ChemBio3D and Chemdraw versions 12) was taken for minimization of energy. The conversion of pdb was done into pdbqt (receptor and ligand file). Autogrid 4 module was used to cover all of the amino acid residues of the protein. The grid dimensions X, Y, Z were set at 90X, 90Y and 90Z Å (receptor axes coordinates), and was allocated the grid space size as 0.375 Å. Lamarckian Genetic Algorithm (LGA) was used for docking simulations in order to turn out the finest conformation of the receptor and the ligand. The docked pose was visualized using PyMOL.

Results

Primarily, so many studies have been focused on unfolding of holo-Mb under different conditions (pH, temperature, denaturants like urea and GdmCl) because of large absorbance changes go with loss of heme and denaturation. Though, result interpretations are indistinct as in most cases heme loss resistance than the apoprotein structure stability is being considered. The concentration of a denaturant is systematically varied in the equilibrium experiments, the concentrations and properties of folded-unfolded and intermediate conformations at equilibrium are observed [46].

GdmCl- and Urea-Induced Mb Denaturation in the Absence and Presence of Ficoll 70 at different pH Values

GdmCl- and urea-induced denaturation of Mb in the presence of ficoll 70 was monitored by observing changes in ε_{409} at different pH values. It has been observed that denaturation of Mb is reversible under these conditions; Y_N (171,000 m^{-1} cm^{-1}) depends on neither pH nor GdmCl and ficoll 70 concentrations; and Y_D measured at different pH values is independent of [GdmCl] in presence of ficoll 70 at all concentrations but shows a slight dependence on pH. Values of $\Delta\varepsilon$ at 409 nm and mean residual ellipticity at 222 nm were plotted as a function of denaturant concentration in order to obtain the transition curves.

Absorption Measurements

The **Figure1** (left panel) shows the changes of $(\varepsilon)_{409}$ values at different pH values (6.0, 7.0 and 8.0) upon GdmCl-induced denaturation in the absence and presence of various concentrations (0, 100, 200 and 300 mg/ml)of ficoll 70. **Figure 2** (left panel) shows the urea-induced denaturation of Mb in the absence and presence of ficoll 70 that has been monitored by using the absorption coefficient (ε) value at 409 nm. It can be seen from the above figures that the pre- and post-transition region are well defined. The protein unfolding was observed to be reversible at all concentration of denaturants in the absence and presence of ficoll 70. The entire data of each denaturation

curve was explored for ΔG_D°, m and C_m by means of non-linear least square method (equation 8). Value of ΔG_D° and C_m of Mb in the native state and in the presence of ficoll 70 were measured and is given in parenthesis in **Table 1.**

Circular Dichroism Measurements

The **Figure 1**(right panel) shows the changes in $[\theta]_{222}$ values at different pH values (6.0, 7.0 and 8.0) upon GdmCl-induced denaturation with and without ficoll 70 (0, 100, 200 and 300 mg/ml) while **Figure 2** (right panel) shows the urea-induced denaturation of Mb with and without ficoll 70, which has been monitored by following the value of mean residual ellipticity at 222 nm. It can be seen that well-defined pre-transition and post-transition regions do exist in the figure. The protein was reversible at all concentration of denaturants in the absence and presence of ficoll 70. The ΔG_D°, m and C_m were analyzed from entire data of each denaturation curve using non-linear least square method (equation 8), ΔG_D° and C_m of Mb in the absence and presence of ficoll 70 were measured and are provided in

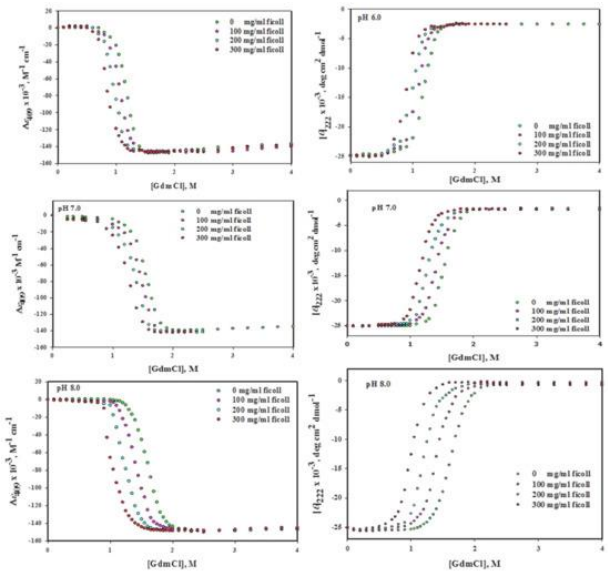

Figure 1: GdmCl-induced denaturation of myoglobin in the absence and presence of different concentrations of ficoll 70 at different pH values.

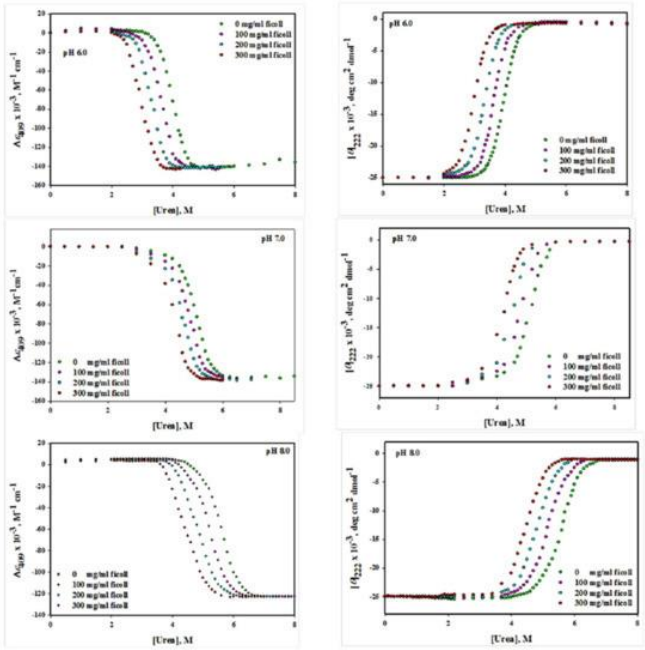

Figure 2. Urea-induced denaturation of myoglobin in the absence and presence of different concentrations of ficoll 70 at different pH values.

Table 1: Thermodynamic parameters of myoglobin in the absence and presence of different concentrations of ficoll 70 at different pH values.

pH	[Ficoll 70] mg/mL	GdmCl-Induced Denaturation		Urea-Induced Denaturation	
		$\Delta G_D°$(kcal mol^{-1})	C_m[M]	$\Delta G_D°$(kcal mol^{-1})	C_m[M]
6	0	10.13 ± 0.11 (10.15 ± 0.12) *	1.26 ± 0.04 (1.25 ± 0.05) *	10.25 ± 0.18 (10.23±0.15) *	3.99 ± 0.05 (4.00 ± 0.04) *
	100	9.70 ± 0.18	1.15 ± 0.06	9.75 ± 0.15	3.60 ± 0.03
	200	9.22 ± 0.12	1.00 ± 0.05	9.31 ± 0.11	3.30 ± 0.04
	300	8.78 ± 0.13	0.95 ± 0.05	8.72 ± 0.10	3.07 ± 0.06
7	0	11.10 ± 0.14 (11.13 ± 0.16) *	1.53 ± 0.03 (1.56 ± 0.02) *	10.95 ± 0.15 (10.98 ± 0.13) *	5.10 ± 0.04 (5.09 ± 0.05) *
	100	10.34 ± 0.15	1.4 ± 0.04	10.38 ± 0.16	4.63 ± 0.05
	200	9.87 ± 0.11	1.2 ± 0.05	9.87 ± 0.14	4.15 ± 0.06
	300	9.08 ± 0.14	1.1 ± 0.03	9.11 ± 0.13	3.58 ± 0.04
8	0	10.23 ± 0.15 (10.21 ± 0.13) *	1.82 ± 0.04 (1.81 ± 0.03) *	10.25 ± 0.11 (10.23 ± 0.14) *	5.83 ± 0.04 (5.85 ± 0.03) *
	100	9.76 ± 0.11	1.7 ± 0.03	9.71 ± 0.18	5.46 ± 0.05
	200	9.28 ± 0.13	1.65 ± 0.04	9.28 ± 0.13	5.04 ± 0.05
	300	8.81 ± 0.14	1.60 ± 0.05	8.81 ± 0.16	4.75 ± 0.06

* Values given in parenthesis are from $\Delta\varepsilon_{409}$ measurements. '±' sign with each parameter represents the mean error obtained from the triplicate measurements.

GdmCl-Induced and Urea-Induced Denaturation of Mb in the Absence and Presence of Dextran 70 at different pH Values

Absorption Measurements

The **Figure 3** (left panel) shows GdmCl-induced denaturation of Mb at pH values 6.0, 7.0 and 8.0 in the absence and presence of different concentrations of dextran 70 (0, 100, 200 and 300 mg/ml). This figure shows the changes in $(\varepsilon)_{409}$ values against the each concentration of GdmCl in absence and presence of dextran 70. **Figure 4** (left panel) shows the changes in $(\varepsilon)_{409}$ of Mb due to urea-induced denaturation in the presence dextran 70 at different concentrations (0-300 mg/ml) under various pH conditions (6.0, 7.0 and 8.0). It can be seen that well-defined pre-transition and post-transition regions do exist in this figure. The unfolding of proteins was found to be reversible at all concentration of denaturants in the absence and presence of dextran70. The ΔG_D°, m and C_m were analyzed from the entire data of each denaturation curve using non-linear least square method (equation 8). Value of ΔG_D° and C_m of GdmCl and urea denatured Mb in the presence of different concentrations of dextran 70 (0-300 mg ml^{-1}) at different pH values are given in

Table 2: Thermodynamic parameters of myoglobin in the absence and presence of different concentrations of dextran 70 at different pH values.

pH	[Dextran 70] mg/mL	GdmCl-Induced Denaturation		Urea-Induced Denaturation	
		$\Delta G_D°$(kcal mol^{-1})	C_m[M]	$\Delta G_D°$(kcal mol^{-1})	C_m[M]
6	0	10.13 ± 0.11 (10.15 ± 0.12) *	1.26 ± 0.04 (1.25 ± 0.05) *	10.25 ± 0.18 (10.23±0.15) *	3.99 ± 0.05 (4.00 ± 0.04) *
	100	9.85 ± 0.15 (9.85 ± 0.14) *	1.04 ± 0.02 (1.05 ± 0.03) *	9.88 ± 0.13 (9.83 ± 0.12) *	3.60 ± 0.03 (3.65 ± 0.02) *
	200	9.44 ± 0.14 (9.43 ± 0.13) *	0.98 ± 0.02 (0.98 ± 0.03) *	9.34 ± 0.14 (9.31 ± 0.12) *	3.10 ±0.02 (3.13 ± 0.03) *
	300	9.05 ± 0.13 (9.05 ± 0.14) *	0.85 ± 0.03 (0.85 ± 0.02) *	9.11 ± 0.13 (9.10 ± 0.14) *	3.70 ± 0.03 (3.71 ± 0.02) *
7	0	11.10 ± 0.14 (11.13 ± 0.16) *	1.53 ± 0.03 (1.56 ± 0.02) *	10.95 ± 0.15 (10.98 ± 0.13) *	5.10 ± 0.04 (5.09 ± 0.05) *
	100	10.55 ± 0.13 (10.57 ± 0.16) *	1.47 ± 0.02 (1.46 ± 0.03) *	10.53 ± 0.16 (10.52 ± 0.18) *	4.71 ± 0.03 (4.70 ± 0.03) *
	200	10.11 ± 0.12 (10.10 ± 0.11) *	1.35 ± 0.01 (1.34 ± 0.04) *	10.17 ± 0.14 (10.14 ± 0.13) *	4.34 ± 0.03 (4.35 ± 0.02) *
	300	9.68 ± 0.13 (9.65 ± 0.12) *	1.15 ± 0.03 (1.16 ± 0.02) *	9.72 ± 0.13 (9.69 ± 0.12) *	4.07 ± 0.02 (4.08 ± 0.03) *
8	0	10.23 ± 0.15 (10.21 ± 0.13) *	1.82 ± 0.04 (1.81 ± 0.03) *	10.25 ± 0.11 (10.23 ± 0.14) *	5.83 ± 0.04 (5.85 ± 0.03) *
	100	9.84 ± 0.14 (9.84 ± 0.16) *	1.58 ± 0.03 (1.59 ± 0.02) *	9.85 ± 0.13 (9.84 ± 0.15) *	4.95 ± 0.02 (4.93 ± 0.03) *
	200	9.40 ± 0.11 (9.43 ± 0.13) *	1.36 ± 0.02 (1.35 ± 0.02) *	9.42 ± 0.15 (9.45 ± 0.13) *	4.61 ± 0.02 (4.62 ± 0.03) *
	300	9.03 ± 0.12 (9.01 ± 0.14) *	1.01 ± 0.03 (1.00 ± 0.02) *	9.04 ± 0.17 (9.06 ± 0.14) *	4.46 ± 0.02 (4.44 ± 0.02) *

* Values given in parenthesis are from $[\theta]_{222}$ measurements. '±' sign with each parameter represents the mean error obtained from the triplicate measurements.

Table 3: Thermodynamic parameters for the binding of dextran 70 and ficoll 70 to myoglobin at pH 7.0 and 25 °C.

Crowder	N	K_a(M^{-1})	ΔH(cal mol^{-1})	ΔS(cal K^{-1} mol^{-1})	K_d(μM)	ΔG(kcal mol^{-1})
Dextran 70	0.74 ± 0.04	10.6×10^5 (± 0.88×10^5)	−1.95 (± 0.16)	−42.5 (± 0.3)	9.43	−6.83
Ficoll 70	[0.71 (± 0.04)] #	[9.42×10^4 (± 1.08×10^4)] #	[-2.93×10^4 (± 0.50×10^4)] #	[−45.4 (± 0.40)] #	[10.62] #	[−15.77] #

Circular Dichroism Measurements

The **Figure3** (right panel) shows GdmCl-induced denaturation of Mb at pH values of 6.0, 7.0 and 8.0, in the absence and presence of different concentrations of dextran 70 (0, 100, 200 and 300 mg/ml). This figure show the changes of $[\theta]_{222}$ values against the each concentration of GdmCl in absence and presence of dextran 70. **Figure 4** (right panel) shows the urea-induced denaturation of Mb at pH values (6.0, 7.0 and 8.0), in the absence and presence of dextran 70 monitoring the mean residual ellipticity at 222 nm. The pre-transition and post-transition regions in the figure are well defined. The protein was found to be reversible at all denaturant concentrations in the absence and presence of dextran 70. ΔG_D°, m and C_m were analyzed from denaturation curves using non-linear least square method (equation 8). Value of ΔG_D° and C_m of GdmCl- and urea-induced denatured Mb in the presence of different concentrations of dextran 70 (0-300 mg ml^{-1}) at different pH values given in parenthesis in **Table 2.**

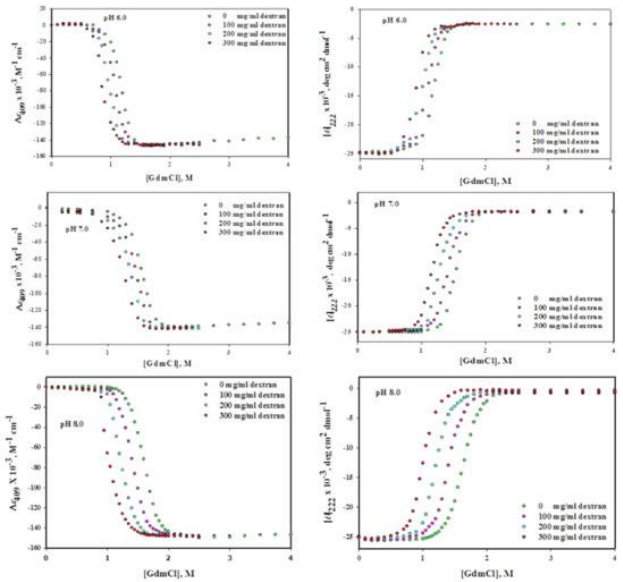

Figure 3: GdmCl-induced denaturation of myoglobin in the absence and presence of different concentrations of dextran 70 at different pH values.

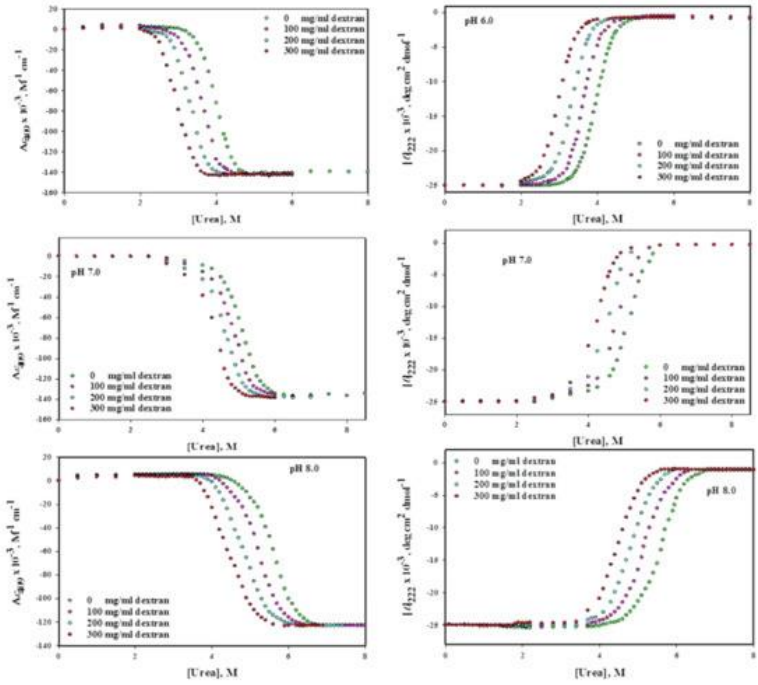

Figure 4: Urea-induced denaturation of myoglobin in the absence and presence of different concentrations of dextran 70 at different pH values.

Interaction Studies

Isothermal Titration Calorimetry Measurements

Earlier, we have reported that ficoll 70 binds with Mb [47]. To know whether the dextran 70 also binds to Mb; and to delineate the chemical basis of structural changes in Mb due to dextran 70, isothermal titration calorimetry (ITC) was carried out to find out possible binding between Mb and dextran 70. Mb in the syringe was titrated inside the cell having dextran 70 (**Figure 5**). The upper panel of this figure shows power versus time after injection of Mb in cell having dextran 70. The figure shows power per mole of the injectant (kcal mol^{-1}) versus its molar ratio at lower panel side. During titrations of Mb into dextran 70 the initial injections produces large negative enthalpic change that reduced upon further addition of Mb into dextran 70. MicroCal Origin ITC software was use to analyze the ITC data.

The binding model, which could fit to the data, was "oneSite" binding model. This binding model was used in order to find out thermodynamic parameter i.e., the association constant (K_a), binding enthalpy (ΔH) and stoichiometry (N). The values of the association constant (K_a),change in entropy (ΔS), Gibb's free energy change (ΔG), binding enthalpy (ΔH) and stoichiometry (N) for dextran 70 binding to Mb are given in **Table 4**. This binding model presumes that one or additional ligand molecule binds with equivalent affinities to a single site. The result from ITC suggests that interaction occurs between dextran 70 and Mb.

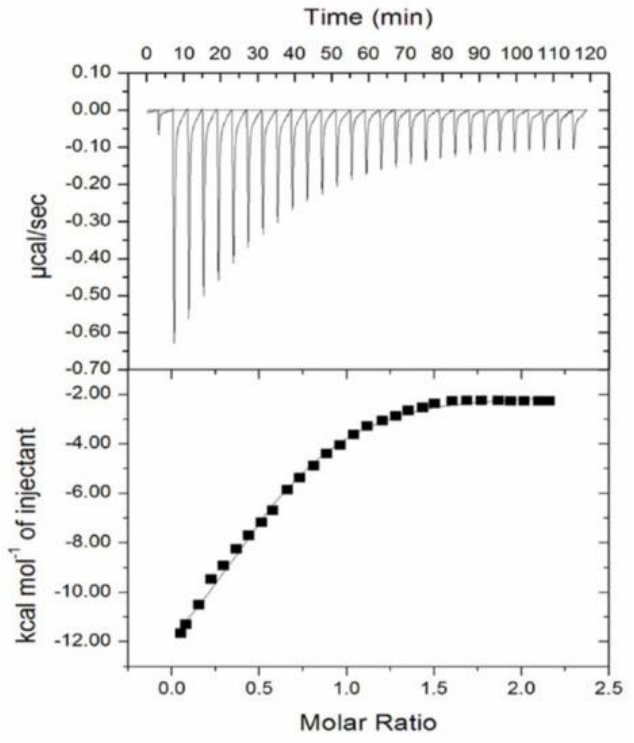

Figure 5: Isothermal titration calorimetry profile for titration of dextran 70 into myoglobin.

Table 4. Comparison of $\Delta\Delta G_D°$ of myoglobin in the presence of 300 mg/mL ficoll 70 and 300 mg/mL dextran 70 at different pH values.

pH	GdmCl-Induced Denaturation		Urea-Induced Denaturation	
	Ficoll 70	Dextran 70	Ficoll 70	Dextran 70
6.0	1.37 ± 0.17	1.1 ± 0.12 (1.08 ± 0.13) *	1.58 ± 0.19	1.12 ± 0.14 (1.15 ± 0.15) *
7.0	1.43 ± 0.20	1.45 ± 0.12 (1.45 ± 0.13) *	1.26 ± 0.19	1.26 ± 0.14 (1.26 ± 0.13) *
8.0	1.6 ± 0.14	1.18 ± 0.12 (1.22 ± 0.14) *	1.62 ± 0.15	1.19 ± 0.16 (1.19 ± 0.13) *

* Values given in parenthesis are from $[\theta]_{222}$ measurements. '±' sign with each parameter represents the mean error obtained from the triplicate measurements.

Molecular Docking Studies

From the ITC studies, we could demonstrate that interaction occurred between the ligand and macromolecule; and measured the thermodynamic parameters associated with binding. However, ITC could not give much information about the mechanism of interaction. To know the basis of interaction and the site where the ligand binds to macromolecule (Mb), molecular docking studies were performed.

The interaction between dextran 70 and Mb was studied by molecular docking using AutoDock4 software. *In-silico* study shows that interaction was significant between myoglobin and dextran 70 as can be seen in **Figure 6**. The computational studies revealed that dextran 70 interacts with the heme of Mb via 1 H-bond. The calculated distance between the two interacting atoms was 2.9 Å. **Figure 7** shows 2D plot of Mb docked with dextran 70 produced by maestro (schrodinger), which depicts metal coordination, bonding, charge, hydrophobicity, polarity etc. on the protein in presence of the ligand. Binding free energy released on interaction of Mb and dextran 70 on docking was calculated to be -3.1 kcal/mol, indicates favorable interactions between Mb and dextran 70. The type of interaction between ficoll 70 and Mb was already reported where molecular docking was performed using AutoDock4 software [47]. *In-silico* study showed that notable interaction existed between Mb and ficoll 70 [47].

Discussions

Thermal- and chemical-induced denaturation of myoglobin is determined by the degree of dissociation of its prosthetic group "heme", which is pursued right away through rapid unfolding of the globule at the high temperatures and concentration of denaturants [48,49]. The resistance of holo-Mb to unfolding depends on intrinsic stability of tertiary structure of the apo-protein and interaction strength of globule with heme. Reason is the affinity of apoMb for heme is enormous ($\approx 3 \times 10^{14}$ M^{-1}), that is so, the holo-protein is more firm to denature than the apoprotein [50-52].

The thermodynamic investigation of protein denaturation is one of the functions for valuation of the stabilization free energy of proteins. It has been defined as the free energy entailed for converting the protein from its native three-dimensional structure to the completely denatured state. The latter state has been observed in concentrated solution of GdmC1, GdmCNS, and urea [53].

Macromolecular crowding has shown great impact on the structure of protein, protein's function, protein stability, protein folding, binding of ligand to protein, protein-protein interaction, molten globule formation and protein aggregation [2,7,9,47,54-59]. Here, the chemical denaturation of Mb was observed under crowding conditions i.e., ficoll 70 and dextran 70, using denaturing agents (GdmCl and urea) at pH values of 6.0, 7.0 and 8.0 at 25 ˚C. Analysis of isothermal transition curves was based on two assumptions: (1) the isothermal denaturation process is reversible and (2) the denaturation process proceeds through two-state mechanism, having equilibrium between

N (native conformation) ↔ **D** (denatured conformation)
Reversible process means that the process of unfolding (from N state to D state) and refolding (from D state to N state) of protein follows the same path. Reversibility of Mb was checked in the absence and presence of each crowder and it was reversible in each case. We have also validated the two state unfolding assumptions of holo-Mb using spectroscopic

techniques (absorption spectroscopy and circular dichroism) in the absence and presence of each crowder. **Tables 1** and **2** show the thermodynamic parameters acquired from GdmCl- and urea-induced denaturation in the presence of each crowder at different concentration (0-300 mg ml^{-1}) using two different probes at different pH values **(Figs 1-4)**. It was observed that the thermodynamic parameters obtained from set of three experiments and from different probes (CD and absorbance) were almost identical and were within the limit of experimental error. This indicates that the process of denaturation proceeds through two-state mechanism, having equilibrium between **N** (native conformation) and **D** (denatured conformation). In this study, reversibility and two-state unfolding mechanism [60-62] is reliable in the absence and presence of crowders. The study of Rahman et. al. [63,64] and Anjum et. al. [65,66] from the same laboratory also reports that the unfolding of Mb at different pH values is a two state reversible process. In the light of earlier finding and this investigation, we conclude that unfolding of Mb is reversible two state processes both in the absence and presence of each crowder at different pH values.

Since the Mb structure is disrupted in the presence of ficoll 70, we wanted to test if the structural effects studied on the native conformation correlate with the Mb stability in the presence of ficoll 70. Although there was no significant effect of dextran 70 on the structure of Mb (Data not shown), we wanted to know whether it has any effect on the stability of Mb or not. In this study, we have monitored the effects of various attributes of macromolecular crowding agents such as effect of shape of crowding agent and nature of the crowding agent on the structure and stability of protein as well as effect of various concentration of crowding agent on the structure and stability of protein. Thus GdmCl- and urea-induced denaturation of Mb was done in variable concentration of ficoll 70 and dextran 70 (0-300 mg ml^{-1}) at three pH values (6.0, 7.0 and 8.0) and at 25 °C. The midpoint of chemical denaturation, C_m and the change in Gibb's free energy $\Delta G_D°$ of a chemical induced denaturation curve for a protein are said to be the most frequently used as protein stability indicator. It was observed from the chemical denaturation curve

of Mb (both urea-induced and GdmCl-induced denaturation) that shift in the transition occurs towards lower denaturant concentration as the concentration of each crowder was increased (**Figs. 1-4; Tables 1-3**). This observation implies that the midpoint of chemical denaturation of Mb decreases with increase in the concentration of each crowding agent. Our aim was to investigate the effect of variable concentrations of each crowder molecule on the values of $\Delta G_D°$ and C_m, which are the key thermodynamic parameters signifying protein stability. The values of $\Delta G_D°$ and C_m of Mb decrease as the concentration of each crowder molecule was increased. The decrease in the value of $\Delta G_D°$ and C_m in the presence of each crowder signifies destabilization of Mb.

Table 3 displays the comparison of thermodynamic stability parameters ($\Delta\Delta G_D°$) of highest concentration of ficoll 70 and dextran 70 effects on Mb. Actually, the value of $\Delta G_D°$ decreases from 11.10 kcal mol^{-1} to 9.08 kcal mol^{-1} upon increasing ficoll 70 concentration from 0 to 300 mg/ml a pH 7.0. In case of dextran 70, the value of $\Delta G_D°$ decreases from 11.10 kcal mol^{-1} to 9.68 kcal mol^{-1} upon increasing the concentration from 0 to 300 mg/ml at pH 7.0. The results at pH 6.0 showed that ficoll 70 (300 mg/ml) decreases the value of $\Delta G_D°$ from 10.13 to 8.78 kcal mol^{-1}. In case of dextran 70 the value of $\Delta G_D°$ decreases from 10.13 kcal mol^{-1} to 9.05 kcal mol^{-1} upon increasing its concentration from 0 to 300 mg/ml at pH 6.0. Similarly at pH 8.0 it was observed that ficoll 70 at concentration of 300 mg/ml decreased the value of $\Delta G_D°$ from 10.23 to 8.81 kcal mol^{-1}. In case of dextran 70, the value of $\Delta G_D°$ decreases from 10.23 to 9.03 kcal mol^{-1} upon increasing its concentration from 0 to 300 mg/ml at pH 8.0. From these observations, it can be suggested that the degree of destabilization was more due to ficoll 70 contrast to that of dextran 70. It is assumed that dextran 70 behaves as rod like structure while ficoll 70 has a spherical structure [67]. It has been reported that dextran 70 owing to its rod like structure excludes greater volume than that of ficoll 70 [68]. But the difference in their structure could not be the reason behind their different degree of destabilization as instead of volume exclusion, here soft interactions are playing a major role. We may hypothesize that ficoll 70 disrupts the tertiary structure of

the protein which lead to greater destabilization than that of dextran 70. Further, there is a clear trend in $\Delta\Delta G_D°$ with respect to both the crowders in these experimental results. It was observed that the degree of destabilization was more due to ficoll 70 than that of dextran 70.

Ficoll 70 is a branched heterogeneous polymer of epichlorohydrin and sucrose while dextran 70 is a branched homogeneous polymer of glucose. Since in the case of soft interactions, chemical interaction are happening, it may be suggested that the nature of crowding agent can be a significant factor in the degree of destabilization of proteins. Crowding agents i.e. low molecular size PEG 400 Da and intermediate sizes (PEG 10 kDa, PEG 8 kDa) [4,58,59], ficoll, dextran [34], proteins (lysozyme and BSA) [4] also destabilizes Mb and in another report it shows that glucose, an osmolyte, also destabilizes Mb [69]. However, it was reported that glucose and sucrose, the monomeric constituents of dextran and ficoll-based crowder prevents the heme dissociation at higher concentrations [4]. Thus, the Crowder's geometry may have ambiguous effects on Mb, in case of soft interactions. We may take liberty to generalize that crowding agent may destabilize Mb irrespective of the nature of crowder or the shape and size of crowder. However, we can safely conclude that the stability of native state of proteins may be depending on other aspects, in addition, to the excluded volume effects due to crowders.

Moreover, we should put emphasis on the point that ficoll 70 disrupts the structure of Mb by disrupting the heme polypeptide interaction, which in turn might be responsible for the reduction in its stability. In addition, after analyzing the result with respect to pH's, it was found that the extent of destabilization is pH dependent i.e. destabilization is greater at pH 7.0 as compared to pH 6.0 and 8.0.

It had been observed that preferential binding of additives leads to destabilization of the protein [29,70-72]. We were interested to know whether the observed destabilization of Mb (in the presence of ficoll 70 or dextran 70) and structure disruption (due to ficoll 70) were due to protein-crowder interaction. To confirm

this statement, ITC measurements were and molecular docking experiments were done. ITC measurements showed that ficoll 70 and dextran 70 interacted with Mb (**Figure 5**) [47]. Earlier, we have shown that apoMb do not binds to ficoll 70, which confirms that ficoll 70 and dextran 70 are interacting with the heme moiety of Mb [47]. The ITC data was fitted through "oneSite" binding model. The binding parameter values given in **Table 4** shows that total change in ΔH and ΔG is negative hence binding of Dextran to the protein is exothermic and spontaneous and the large value of K_a and smaller K_d shows binding is strong. The values from the **Table 4** shows that binding is greater between dextran 70 and Mb, where *K*a value is greater than the K_a of ficoll 70 and Mb. This binding model presumes that one or additional ligand molecule binds with equivalent affinity at single site. This result suggests clear interaction between ficoll 70 and Mb within the confines of this experiment.

Earlier work shows that H-bond length between ficoll 70 and heme is 1.8 and 2.3 Å while the H-bond distance of ficoll 70 with serine 92 is 2.8 Å [47]. It is believed that H-bond distance with donor-acceptor in the range of 1.8–2.3 Å as "strong, while distance in the range of 2.5–3.2 Å as "weak or moderate [73]. Ficoll 70 was shown to bind with Mb at average binding energy of −3.9 kcal/mol. Ficoll 70 alters the conformation of Mb and leads to the reduction in its stability. Ficoll 70 interacts with heme via two strong hydrogen bonds and does not interact with polypeptide chain of Mb but with Ser 92 of it [47]. Sankaranarayanan et al. had showed interaction of ficoll 70 with Serine residue of fibrinogen [74]. To seek into the binding mechanism of dextran 70 with Mb, molecular docking studies were performed. The computational studies revealed that dextran 70 interacts with the heme of Mb via 1 H-bond (**Figure 6**). The calculated distance between the two interacting atoms was 2.9 Å. Binding free energy released on interaction of Mb and dextran 70 on docking was calculated to be -3.1 kcal/mol, indicates favorable interactions between Mb and dextran 70. **Figure 7** shows 2D plot of docked Mb with dextran. This 2D plot was generated by maestro (Schrodinger) shows metal coordination, bonding, charge, hydrophobicity, polarity etc. on the protein in presence of the ligand.

Zhang et al. was first to report that different crowder molecules have dissimilar effects on human apo α-lactalbumin (apo-HLA) stability and structure i.e. ficoll 70 increased the stability to some extent, dextran 70 significantly increased the stability whereas PEG 2000 led to destabilization of apo-HLA protein. Moreover, they also observed that neither ficoll 70 nor dextran 70 interacts with apo-HLA but weak interaction was observed between PEG 2000 and apo-HLA. It was hypothesized as if the weak non-specific interaction is overcoming the effect of volume exclusion and thus leading to destabilization of apo-HLA protein.

The structure, stability and function of protein are regulated by balance between all the acting forces (either attractive or repulsive), between the solvent and the unfolded or folded state of protein. The hydrophobic side chains exposed towards solvent in case of the unfolded conformation of protein. When the solvent or co-solute molecule interacts favorably to the exposed hydrophobic group then the unfolded molecule will be more stabilized which leads to decrease of the T_m [75,76].

Understanding of the intracellular environment requires information about how the proteins are affected in the crowded intra-cellular milieu. The effect of crowding [77] arises due to steric repulsions and chemical interactions [78,79]. The crowding effect on the stability of protein mainly focuses on hard core repulsion, which is mainly stabilizing and entropic in nature. Wang et. al. investigated this phenomena by calculating the NMR detected amide proton exchange dependence on temperature and utilized these data in order to find out the enthalpic and entropic contribution due to crowding in case of ubiquitin [80]. Unexpectedly it was observed that the chemical interaction contribution is huge; and in most of the cases it dominates the hard core repulsion contribution. They have shown that both hard core repulsion and chemical interaction should be considered while investigating the crowding effects. The hardcore repulsion leads to decrease of the available space to proteins. Le Chatelier's principle led us to conclude that the repulsive force favors the native state since this state is more compacted than that of the denatured state. Hardcore repulsion is completely entropic in nature since it includes only

molecular rearrangement and no interaction. The original concept of macromolecular crowding [81] and massive work in this area has provided importance only to hardcore repulsions however, Interactions can be attractive or repulsive. The repulsive interaction stabilizes the protein because it strengthens the hardcore repulsion. The attractive interaction destabilizes the proteins e.g. urea interacts with protein leading to their destabilization. Non-specific and favorable interaction with the backbone of protein leads to surface exposure leading to its unfolding. Attractive interactions have enthalpic component [82]. Information regarding the relative effect of chemical interaction and hardcore repulsion is very less because very few studies have shown the effect of crowding on $\Delta S_D°$ and $\Delta H_D°$. Crowding stabilizes proteins since native state is favored due to hardcore repulsion. Crowding increases $\Delta G_D°$ because $\Delta S_D°$ gets decreased while $\Delta H_D°$ remains constant. We can articulate that interactions between macromolecules and ligands are an important part in macromolecular crowding to investigate for the protein stability.

Conclusion

In this work, the main aim was to know the reason behind the unique behavior of ficoll 70 and dextran 70 towards Mb. It was observed that the degree of destabilization of Mb was greater due to ficoll 70 as compared to that of dextran 70 and was irrespective of the nature of crowder or the shape of crowder (qualitatively independent while quantitatively dependent). The degree of destabilization was observed pH dependent i.e. destabilization is greater at pH 7.0 as compared to pH 6.0 and 8.0. From ITC and computational analysis it was confirmed that both the crowders (ficoll 70 and dextran 70) bind to heme moiety of Mb and single binding site was observed for each. This study advocates that excluded volume effect is not the only leading factor that determines the conformation of proteins in crowded environment. Soft interactions may also play major role in macromolecular crowded environment as far as the stability of a protein is concerned.

References

1. RJ Ellis. Macromolecular crowding: obvious but underappreciated. Trends Biochem Sci. 2001; 26: 597-604.
2. HX Zhou, G Rivas, AP Minton. Macromolecular crowding and confinement: biochemical, biophysical, and potential physiological consequences. Annu Rev Biophys. 2008; 37: 375-397.
3. ZA Parray, S Shahid, F Ahmad, MI Hassan, A Islam. Characterization of intermediate state of myoglobin in the presence of PEG 10 under physiological conditions. Int J Biol Macromol. 2017; 99: 241-248.
4. J Kundu, U Kar, S Gautam, S Karmakar, PK Chowdhury. Unusual effects of crowders on heme retention in myoglobin. FEBS Lett. 2015; 589: 3807-3815.
5. DS Goodsell. Inside a living cell. Trends in Biochemical Sciences. 1991; 16: 203-206.
6. A Samiotakis, P Wittung-Stafshede, MS Cheung. Folding, stability and shape of proteins in crowded environments: experimental and computational approaches. Int J Mol Sci. 2009; 10: 572-588.
7. IM Kuznetsova, KK Turoverov, VN Uversky. What Macromolecular Crowding Can Do to a Protein. International Journal of Molecular Sciences. 2014; 15: 23090-23140.
8. J Batra, K Xu, HX Zhou. Nonadditive effects of mixed crowding on protein stability. Proteins. 2009; 77: 133-138.
9. K Sasahara, P McPhie, AP Minton. Effect of dextran on protein stability and conformation attributed to macromolecular crowding. J Mol Biol. 2003; 326: 1227-1237.
10. L Stagg, SQ Zhang, MS Cheung, P Wittung-Stafshede. Molecular crowding enhances native structure and stability of alpha/beta protein flavodoxin. Proc Natl Acad Sci U S A. 2007; 104: 18976-18981.
11. M Perham, L Stagg, P Wittung-Stafshede. Macromolecular crowding increases structural content of folded proteins. FEBS Lett. 2007; 581: 5065-5069.
12. R Engel, AH Westphal, DH Huberts, SM Nabuurs, S Lindhoud, et al. Macromolecular crowding compacts

unfolded apoflavodoxin and causes severe aggregation of the off-pathway intermediate during apoflavodoxin folding. J Biol Chem. 2008; 283: 27383-27394.
13. D Homouz, M Perham, A Samiotakis, MS Cheung, P Wittung-Stafshede. Crowded, cell-like environment induces shape changes in aspherical protein. Proc Natl Acad Sci U S A. 2008; 105: 11754-11759.
14. Y Wang, H He, S Li. Effect of Ficoll 70 on thermal stability and structure of creatine kinase. Biochemistry (Mosc). 2010; 75: 648-654.
15. T Mikaelsson, J Aden, LB Johansson, P Wittung-Stafshede. Direct observation of protein unfolded state compaction in the presence of macromolecular crowding. Biophys J. 2013; 104: 694-704.
16. J Aden, P Wittung-Stafshede. Folding of an unfolded protein by macromolecular crowding in vitro. Biochemistry. 2014; 53: 2271-2277.
17. OV Stepanenko, OI Povarova, AI Sulatskaya, LA Ferreira, BY Zaslavsky, et al. Protein unfolding in crowded milieu: what crowding can do to a protein undergoing unfolding? Journal of Biomolecular Structure and Dynamics. 2015; 1-16.
18. S Mittal, LR Singh. Denatured state structural property determines protein stabilization by macromolecular crowding: a thermodynamic and structural approach. PLoS One. 2013; 8: e78936.
19. I Pozdnyakova, P Wittung-Stafshede. Non-linear effects of macromolecular crowding on enzymatic activity of multi-copper oxidase. Biochim Biophys Acta. 2010; 1804: 740-744.
20. GS Sharma, S Mittal, LR Singh. Effect of Dextran 70 on the thermodynamic and structural properties of proteins. Int J Biol Macromol. 2015; 79: 86-94.
21. J Zhu, H He, S Li. Macromolecular Crowding Enhances Thermal Stability of Rabbit Muscle Creatine Kinase. Tsinghua Science & Technology. 2008; 13: 454-459.
22. JM Yuan, CL Chyan, HX Zhou, TY Chung, H Peng, et al. The effects of macromolecular crowding on the mechanical stability of protein molecules. Protein Science: A Publication of the Protein Society. 2008; 17: 2156-2166.

23. MS Cheung, D Klimov, D Thirumalai. Molecular crowding enhances native state stability and refolding rates of globular proteins. Proc Natl Acad Sci U S A. 2005; 102: 4753-4758.
24. D Homouz, L Stagg, P Wittung-Stafshede, MS Cheung. Macromolecular crowding modulates folding mechanism of alpha/beta protein apoflavodoxin. Biophys J. 2009; 96: 671-680.
25. A Christiansen, Q Wang, A Samiotakis, MS Cheung, P Wittung-Stafshede. Factors defining effects of macromolecular crowding on protein stability: an in vitro/in silico case study using cytochrome c. Biochemistry. 2010; 49: 6519-6530.
26. A Christiansen, P Wittung-Stafshede. Quantification of excluded volume effects on the folding landscape of Pseudomonas aeruginosa apoazurin in vitro. Biophys J. 2013; 105: 1689-1699.
27. DL Zhang, LJ Wu, J Chen, Y Liang. Effects of macromolecular crowding on the structural stability of human alpha-lactalbumin. Acta Biochim Biophys Sin (Shanghai). 2012; 44: 703-711.
28. LA Benton, AE Smith, GB Young, GJ Pielak. Unexpected effects of macromolecular crowding on protein stability. Biochemistry. 2012; 51: 9773-9775.
29. M Senske, L Törk, B Born, M Havenith, C Herrmann, S Ebbinghaus. Protein Stabilization by Macromolecular Crowding through Enthalpy Rather Than Entropy. Journal of the American Chemical Society. 2014; 136: 9036-9041.
30. SR Kulothungan, M Das, M Johnson, C Ganesh, R Varadarajan. Effect of crowding agents, signal peptide, and chaperone SecB on the folding and aggregation of E. coli maltose binding protein. Langmuir. 2009; 25: 6637-6648.
31. DS Spencer, K Xu, TM Logan, HX Zhou. Effects of pH, salt, and macromolecular crowding on the stability of FK506-binding protein: an integrated experimental and theoretical study. J Mol Biol. 2005; 351: 219-232.
32. DC Kuhnert, S Gildenhuys, HW Dirr. Effect of macromolecular crowding on the stability of monomeric glutaredoxin 2 and dimeric glutathione transferase A1-1. South African Journal of Science. 2008; 104: 76-80.

33. X Aguilar, FW C, T Sparrman, M Wolf-Watz, P Wittung-Stafshede. Macromolecular crowding extended to a heptameric system: the Co-chaperonin protein 10. Biochemistry. 2011; 50: 3034-3044.
34. A Malik, J Kundu, SK Mukherjee, PK Chowdhury. Myoglobin Unfolding in Crowding and Confinement. Journal of Physical Chemistry B. 2012; 116: 12895-12904.
35. I Haque, A Islam, R Singh, AA Moosavi-Movahedi, F Ahmad. Stability of proteins in the presence of polyols estimated from their guanidinium chloride-induced transition curves at different pH values and 25 degrees C. Biophys Chem. 2006; 119: 224-233.
36. Y Goto, N Takahashi, AL Fink. Mechanism of acid-induced folding of proteins. Biochemistry. 1990; 29: 3480-3488.
37. D Puett, W ttaoE Friebele, BK Wasserman. The Equilibrium Unfolding Parameters of Horse and Sperm Whale Myoglobin: EFFECTS OF GUANIDINE HYDROCHLORIDE, UREA, AND ACID. Journal of Biological Chemistry. 1973; 248: 4623-4634.
38. Y Nozaki. The preparation of guanidine hydrochloride. Methods Enzymol. 1972; 26: 43-50.
39. CN Pace. Determination and analysis of urea and guanidine hydrochloride denaturation curves. Methods Enzymol. 1986; 131: 266-280.
40. P Hagel, JJT Gerding, W Fieggen, H Bloemendal. Cyanate formation in solutions of urea: I. Calculation of cyanate concentrations at different temperature and pH. Biochimica et Biophysica Acta (BBA) - Protein Structure. 1971; 243: 366-373.
41. GR Stark. Reactions of cyanate with functional groups of proteins. IV. Inertness of aliphatic hydroxyl groups. Formation of carbamyl- and acylhydantoins. Biochemistry. 1965; 4: 2363-2367.
42. W Fissell, CL Hofmann, R Smith, MH Chen. Size and conformation of Ficoll as determined by size-exclusion chromatography followed by multiangle light scattering. Am J Physiol Renal Physiol. 2010; 298: 21.
43. A Technologies. A guide to multi-detector gel permeation chromatography, in. 2012.

44. NJ Greenfield. Using circular dichroism spectra to estimate protein secondary structure. Nature protocols. 2006; 1: 2876-2890.
45. GM Morris, R Huey, W Lindstrom, MF Sanner, RK Belew, et al. AutoDock4 and AutoDockTools4: Automated Docking with Selective Receptor Flexibility. Journal of computational chemistry. 2009; 30: 2785-2791.
46. TE Creighton. Characterizing intermediates in protein folding. Curr Biol. 1991; 1: 8-10.
47. K Nasreen, S Ahamad, F Ahmad, MI Hassan, A Islam. Macromolecular crowding induces molten globule state in the native myoglobin at physiological pH. Int J Biol Macromol. 2018; 106: 130-139.
48. QH Gibson, E Antonini. Kinetic studies on the reaction between native globin and haem derivatives. Biochem J. 1960; 77: 328-341.
49. MY Rose, JS Olson. The kinetic mechanism of heme binding to human apohemoglobin. J Biol Chem. 1983; 258: 4298-4303.
50. YV Griko, PL Privalov, SY Venyaminov, VP Kutyshenko. Thermodynamic study of the apomyoglobin structure. J Mol Biol. 1988; 202: 127-138.
51. FM Hughson, RL Baldwin. Use of site-directed mutagenesis to destabilize native apomyoglobin relative to folding intermediates. Biochemistry. 1989; 28: 4415-4422.
52. MS Hargrove, S Krzywda, AJ Wilkinson, Y Dou, M Ikeda-Saito, et al. Stability of myoglobin: a model for the folding of heme proteins. Biochemistry. 1994; 33: 11767-11775.
53. C Tanford. Protein denaturation. C. Theoretical models for the mechanism of denaturation. Adv Protein Chem. 1970; 24: 1-95.
54. AP Minton. The effect of volume occupancy upon the thermodynamic activity of proteins: some biochemical consequences. Mol Cell Biochem. 1983; 55: 119-140.
55. AP Minton. How can biochemical reactions within cells differ from those in test tubes? J Cell Sci. 2006; 119: 2863-2869.
56. AP Minton. Implications of macromolecular crowding for protein assembly. Curr Opin Struct Biol. 2000; 10: 34-39.

57. AP Minton. Effect of a concentrated "inert" macromolecular cosolute on the stability of a globular protein with respect to denaturation by heat and by chaotropes: a statistical-thermodynamic model. Biophys J. 2000; 78: 101-109.
58. ZA Parray, S Shahid, F Ahmad, MI Hassan, A Islam. Characterization of intermediate state of myoglobin in the presence of PEG 10 under physiological conditions. Int J Biol Macromol. 2017; 99: 241-248.
59. ZA Parray, S Ahamad, F Ahmad, MI Hassan, A Islam. First evidence of formation of pre-molten globule state in myoglobin: A macromolecular crowding approach towards protein folding in vivo. International Journal of Biological Macromolecules. 2019; 126: 1288-1294.
60. R Gupta, S Yadav, F Ahmad. Protein Stability: Urea-Induced versus Guanidine-Induced Unfolding of Metmyoglobin. Biochemistry. 1996; 35: 11925-11930.
61. A Malik, J Kundu, SK Mukherjee, PK Chowdhury. Myoglobin Unfolding in Crowding and Confinement. The Journal of Physical Chemistry B. 2012; 116: 12895-12904.
62. I Nishii, M Kataoka, Y Goto. Thermodynamic stability of the molten globule states of apomyoglobin. J Mol Biol. 1995; 250: 223-238.
63. S Rahman, SA Ali, A Islam, MI Hassan, F Ahmad. Data on the role of accessible surface area on osmolytes-induced protein stabilization. Data in Brief. 2017; 10: 47-56.
64. S Rahman, SA Ali, A Islam, MI Hassan, F Ahmad. Testing the dependence of stabilizing effect of osmolytes on the fractional increase in the accessible surface area on thermal and chemical denaturations of proteins. Arch Biochem Biophys. 2016; 591: 7-17.
65. V Rishi, F Anjum, F Ahmad, W Pfeil. Role of non-compatible osmolytes in the stabilization of proteins during heat stress. Biochem J. 1998; 329: 137–143.
66. F Anjum, V Rishi, F Ahmad. Compatibility of Osmolytes with Gibbs Energy of Stabilization of Proteins. Biochim Biophys Acta. 2000; 1476: 75-84.
67. L Homchaudhuri, N Sarma, R Swaminathan. Effect of crowding by dextrans and Ficolls on the rate of alkaline phosphatase-catalyzed hydrolysis: a size-dependent investigation. Biopolymers. 2006; 83: 477-486.

68. S Shahid, MI Hassan, A Islam, F Ahmad. Size-dependent studies of macromolecular crowding on the thermodynamic stability, structure and functional activity of proteins: in vitro and in silico approaches. Biochim Biophys Acta. 2017; 1861: 178-197.
69. Y You, F Liu, KJ Du, GB Wen, YW Lin. Structural and functional alterations of myoglobin by glucose-protein interactions. Journal of Molecular Modeling. 2014; 20: 2358.
70. A Malik, J Kundu, SK Mukherjee, PK Chowdhury. Myoglobin unfolding in crowding and confinement. J Phys Chem B. 2012; 116: 12895-12904.
71. LA Benton, AE Smith, GB Young, GJ Pielak. Unexpected Effects of Macromolecular Crowding on Protein Stability. Biochemistry. 2012; 51: 9773-9775.
72. M Jiao, HT Li, J Chen, AP Minton, Y Liang. Attractive Protein-Polymer Interactions Markedly Alter the Effect of Macromolecular Crowding on Protein Association Equilibria. Biophysical Journal. 2010; 99: 914-923.
73. JJ Dannenberg. An Introduction to Hydrogen Bonding By George A. Jeffrey (University of Pittsburgh). Oxford University Press: New York and Oxford. 1997. ix + 303 pp. $60.00. ISBN 0-19-509549-9, Journal of the American Chemical Society. 1998; 120: 5604-5604.
74. K Sankaranarayanan, N Meenakshisundaram. Influence of Ficoll on urea induced denaturation of fibrinogen. AIP Advances. 2016; 6: 035130.
75. JC Lee, LL Lee. Preferential solvent interactions between proteins and polyethylene glycols. J Biol Chem. 1981; 256: 625-631.
76. LLY Lee, JC Lee. Thermal stability of proteins in the presence of poly(ethylene glycols). Biochemistry. 1987; 26: 7813-7819.
77. AP Minton, J Wilf. Effect of macromolecular crowding upon the structure and function of an enzyme: glyceraldehyde-3-phosphate dehydrogenase. Biochemistry. 1981; 20: 4821-4826.
78. AH Elcock. Models of macromolecular crowding effects and the need for quantitative comparisons with experiment. Curr Opin Struct Biol. 2010; 20: 196-206.

79. SR McGuffee, AH Elcock. Diffusion, Crowding & Protein Stability in a Dynamic Molecular Model of the Bacterial Cytoplasm. PLOS Computational Biology. 2010; 6: e1000694.
80. Y Wang, M Sarkar, AE Smith, AS Krois, GJ Pielak. Macromolecular Crowding and Protein Stability. Journal of the American Chemical Society. 2012; 134: 16614-16618.
81. AP Minton. Excluded volume as a determinant of macromolecular structure and reactivity. Biopolymers. 1981; 20: 2093-2120.
82. GI Makhatadze, PL Privalov. Protein interactions with urea and guanidinium chloride. A calorimetric study. J Mol Biol. 1992; 226: 491-505.